# Characteristics and mathematical models of the thin-layer drying of paddy rice with low-pressure superheated steam

Yan Li[1], Gang Che[1,2*], Lin Wan[1], Qilin Zhang[1], Tianqi Qu[1], Fengzhou Zhao[3]

(1. *College of Engineering, Heilongjiang Bayi Agricultural University, Daqing 163319, Heilongjiang, China*;
2. *Heilongjiang Key Laboratory of Intelligent Agricultural Machinery Equipment, Daqing 163319, Heilongjiang, China*;
3. *College of Agriculture, Heilongjiang Bayi Agricultural University, Daqing 163319, Heilongjiang, China*)

**Abstract:** Drying paddy with low-pressure superheated steam (LPSS) can effectively increase the γ-aminobutyric acid content in paddy. This study aimed to investigate the characteristics and mathematical models (MMs) of thin-layer drying of paddy with LPSS. The experimentally obtained data were fitted by nonlinear regression with 5 MMs commonly used for thin-layer drying to calculate the goodness of fit of the MMs. Then, the thin-layer drying of paddy with LPSS was modeled with two machine learning methods as a Bayesian regularization back propagation (BRBP) neural network and a support vector machine (SVM). The results showed that paddy drying with LPSS is a reduced-rate drying process. The drying temperature and operating pressure have a significant impact on the drying process. Under the same pressure, increasing the drying temperature can accelerate the drying rate. Under the same temperature, increasing the operating pressure can accelerate the drying rate. The comparison of the model evaluation indexes showed that 5 common empirical MMs (Hederson and Pabis, Page, Midilli, Logarithmic, and Lewis) for thin-layer drying can achieve excellent fitting effects for a single experimental condition. However, the regression fitting of the indexes by calculating the coefficient(s) of each model showed that the empirical MMs produce poor fitting effects. The BRBP neural network-based model was slightly better than the SVM-based model, and both were significantly better than the empirical MM (the Henderson and Pabis model), as evidenced by a comparison of the training root mean square error (RMSE), testing RMSE, training mean absolute error (MAE), testing MAE, training $R^2$, and testing $R^2$ of the Henderson and Pabis model, the BRBP neural network model, and the SVM-based model. This results indicate that the MMs established by the two machine learning methods can better predict the moisture content changes in the paddy samples dried by LPSS.

**Keywords:** paddy, low-pressure superheated steam, drying, mathematical model, characteristic
**DOI:** 10.25165/j.ijabe.20231601.7810

**Citation:** Li Y, Che G, Wan L, Zhang Q L, Qu T Q, Zhao F Z. Characteristics and mathematical models of the thin-layer drying of paddy rice with low-pressure superheated steam. Int J Agric & Biol Eng, 2023; 16(1): 273–282.

## 1 Introduction

Rice is one of the most important grains in the world. However, with the development of food diversification, the consumption of rice as a staple food has been decreasing each year. Therefore, functional rice rich in γ-aminobutyric acid (GABA) has become a popular research topic worldwide[1,2]. GABA is a four-carbon nonprotein amino acid that is mainly produced by the conversion of glutamate through catalysis by glutamate decarboxylase (GAD). GABA acts as an inhibitory neurotransmitter in the central nervous system of mammals and participates in the physiological activities of cerebral circulation. GABA has antihypertensive, antiarrhythmic, diuretic, analgesic, and anxiety-relieving effects. GABA insufficiency is closely associated with posttraumatic stress disorder, schizophrenia, fibromyalgia, and other central pain syndromes, and GABA dysfunction is associated with the occurrence of bipolar disorder[3-6]. Li et al.[7] found that the combined use of low-pressure wet steam enrichment and LPSS drying processes can effectively increase the GABA content in rice and that 10% of the total GABA content can be attributed to enrichment in the LPSS drying stage.

LPSS drying combines superheated steam in direct contact with a damp material under low pressure to remove moisture from the material. LPSS can dry a damp material at a relatively low temperature in an oxygen-free environment, which effectively reduce the loss of nutrients by oxidation and thermal degradation during the drying process. Therefore, LPSS can dry material to a suitable moisture level at a relatively low temperature and can ensure a quality appearance and the nutrient composition of the material[8-12]. LPSS has been successful in the drying treatment of agricultural products, such as wood, silk, onion, silkworm cocoon, carrot chunks, and parsley[13-16].

Drying mathematical models (MMs) can be used to optimize drying parameters, design and improve drying equipment, reduce drying energy consumption, and improve drying quality. Currently, there are many LPSS drying models. For example, Elustondo et al.[17] constructed an MM to calculate the process of LPSS drying of food particles. Zhang et al.[18] studied the thin-layer drying characteristics of sludge under superheated steam, constructed MMs, analyzed the thin-layer drying characteristics of sludge under superheated steam, and fitted the data with seven types of thin-layer drying MMs. These results showed that the Midilli model can simulate the superheated steam drying process of sludge well. Li et

**Received date:** 2022-07-19 **Accepted date:** 2022-11-24
**Biographies: Yan Li**, PhD, research interest: drying of typical agricultural products, Email: 864385020@qq.com; **Lin Wan**, Professor, research interest: agricultural mechanization, Email: 381995603@qq.com; **Qilin Zhang**, MS candidate, research interest: drying of typical agricultural products, Email: 278006949@qq.com; **Tianqi Qu**, MS candidate, research interest: drying of typical agricultural products, Email: 474669832@qq.com; **Fengzhou Zhao**, PhD, research interest: plant resistance, Email: 521zhaofengzhou@163.com.
***Corresponding author: Gang Che**, Professor, research interest: intelligent agricultural machinery equipment and typical agricultural products drying. College of Engineering, Heilongjiang Bayi Agricultural University, Daqing 163319, Heilongjiang, China. Tel: +86-13836961617, Email: chegang180@126.com.

al.[19] studied the LPSS drying characteristics of green radish slices and showed that superheated steam produces a faster drying rate. Yuan et al.[20] constructed an MM for the superheated steam drying of *Penaeus vannamei* and showed that the lower superheated steam temperature results in a higher drying quality of *Penaeus vannamei*.

In the research on paddy processing. already researchers have mainly focused on the method of reducing paddy drying costs and the crack ratio. Due to the high cost of LPSS drying of paddy, there are few previous studies on this topic. However, GABA-enriched paddy has high economic value, so increasing the drying cost to improve paddy quality is a worthwhile endeavor. Since LPSS drying can effectively increase the GABA content in paddy, this method was selected for this study.

In this study, the effects of temperature, pressure, and time of LPSS on the moisture content in paddy were analyzed. The experimental data were fitted with five types of thin-layer drying MMs. However, the moisture content of paddy is significantly nonlinear and time-varying during the drying process, and using only a single model to fit the processes under different conditions inevitably limits the adaptability and prediction accuracy. In recent years, machine learning-based MMs have been constructed to predict the relationships between complex process parameters, showing excellent adaptability and predictive power[21-24]. Therefore, a Bayesian regularization backpropagation (BRBP) neural network and a support vector machine (SVM) were used to establish MMs for LPSS drying of paddy, and the results were compared with those of empirical MMs. This study provides a theoretical reference and technical guidance for the application of the LPSS drying technology to paddy.

## 2 Materials and methods

### 2.1 Test materials

Test sample: Suijing-18 japonica rice produced in 2021 was provided by Qing'an Donghe Jingu Grain Reserve Co., Ltd (Harbin, China).

### 2.2 Test equipment

The drying test bench is shown in Figure 1, which is mainly composed of 20 components, including a sealed acrylic box, an aluminum foil heater, a gas superheater, a temperature sensor, a condenser, and a vacuum pump (1550D, Maximum pressure −0.098 MPa, Taizhou Fujiwara Tools Co., Ltd., China).

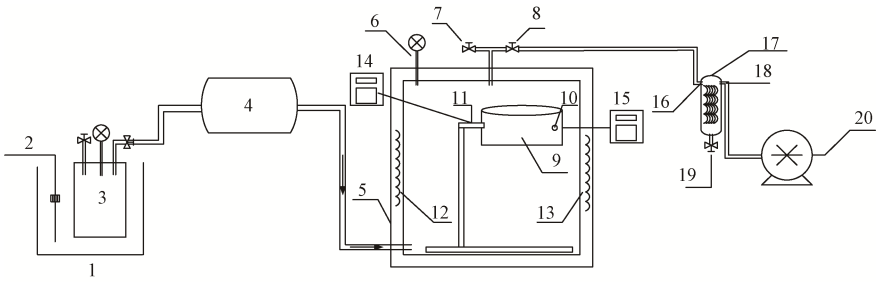


1. Water bathtub 2. Water bath thermostatic heater 3. Vacuum barrel 4. Superheater 5. Drying box 6. Pressure gauge 7. Vent valve 8. Air extraction port 9. Material rack 10. Temperature sensor 11. Medium-weight sensor 12. Aluminum foil heater 13. Aluminum foil heater 14. Weighing system 15. Temperature detection system 16. Condenser air inlet 17. Vapor-water condensate separator 18. Condenser air outlet 19. Drain 20. Vacuum pump

Figure 1 Drying test bench

The other instruments used include an electronic balance (JT1003D, 100 g/0.1 mg, Shanghai Hengji Scientific Instrument Co., Ltd.) and a digital electric thermostatic drying oven (101-A, 300°C/±1°C, Shanghai Jinping Instrument Co., Ltd., China).

In this experiment, the paddy was dried using the LPSS generated by the test bench as shown in Figure 1. An appropriate amount of clean water was placed in the vacuum barrel, and the water bath heater was turned on to heat the vacuum barrel. Then, the gas superheater and the aluminum foil heaters were turned on. Next, the vacuum pump and the cooling tank were turned on. The steam generated in the vacuum barrel reached the superheated state after passing through the gas superheater and the aluminum foil heater.

### 2.3 Test method

#### 2.3.1 Preparation of test samples

Select plump rice grains and place them on the bench., set at an absolute pressure of 0.026 MPa, a temperature of 60.66°C, and a drying time of 5.01 h for the enrichment of GABA in rice. Under these enrichment conditions, the GABA content in rice reached 94.1751 mg/100 g. After the enrichment was completed, the paddy samples were removed and cooled at room temperature (22°C) for 1 h. After cooling, the paddy samples were placed in sealed bags and stored in a refrigerator at 4°C for later use[7]. Two hours before the experiment, the paddy samples were taken out from the refrigerator and placed in an airtight glass container to reach room temperature for further experiments.

#### 2.3.2 Cooperation method and experimental design

The system was preheated according to the specific experimental design temperature, and 100 g samples were taken and placed on the sample rack (10), the parameters of the test bench were adjusted according to the test plan, and steam flow is set at 0.5 L/h, and the test was started, 10 g paddy was sampled every 10 min to measure the moisture content at that time.

The pressure, temperature, and drying time of the test bench were adjusted to (0.01 MPa, 0.015 MPa, 0.02 MPa, 0.025 MPa, or 0.03 MPa), (50°C, 55°C, 60°C, 65°C, or 70°C), and (10 min, 20 min, 30 min, 40 min, 50 min, or 60 min), respectively, to analyze the effects of these parameters on the moisture content of paddy.

#### 2.3.3 Moisture content measurement method

1) Determination of the initial moisture content of the paddy samples

The paddy samples were placed in an electric thermostatic drying oven at 103°C for 40 min.

2) Calculation of the moisture ratio (MR)

The MR of the paddy samples at the drying time $t$ was calculated through Equation (1):

$$\mathrm{MR}=\frac{M_t-M_e}{M_0-M_e} \tag{1}$$

where, MR is the moisture ratio of a paddy sample at time $t$; $M_t$ is the moisture content of the paddy sample at the drying time $t$, %; $M_0$ is the initial moisture content of the paddy sample, %; $M_e$ is the equilibrium moisture content of the paddy sample, %.

There is no equilibrium $M_e$ in superheated steam drying, and the paddy samples can be dried to a very low moisture content. Hence, the equilibrium MR is considered to be zero, and the expression of the MR can be simplified as Equation (2)[25].

$$\mathrm{MR}=\frac{M_t}{M_0} \tag{2}$$

2.3.4 Establishment of drying MMs

1) Establishment of empirical MMs

The data of the LPSS drying experiment were fitted with five common thin-layer drying MMs, and the goodness of fit of the MMs under a single experimental environmental condition was analyzed. The model coefficients under each experimental condition were then calculated and subjected to regression fitting to obtain the overall goodness of fit between each model and the experimental data. The five common MMs analyzed in this study are listed in Table 1[26-28].

**Table 1 Empirical MMs for thin-layer paddy drying**

| Serial number | Model name | Model equation |
|---|---|---|
| 1 | Hederson and Pabis | $\mathrm{MR}=a\exp(-kt)$ |
| 2 | Page | $\mathrm{MR}=\exp(-kt^x)$ |
| 3 | Midilli | $\mathrm{MR}=a\exp(-kt^x)+bt$ |
| 4 | Logarithmic | $\mathrm{MR}=a\exp(-kt)+c$ |
| 5 | Lewis | $\mathrm{MR}=\exp(-kt)$ |

Note: MR is the moisture ratio of a paddy sample, %; $a$, $k$, $x$, $b$, and $c$ are the model coefficients; $t$ is the drying time, s.

2) Establishment of a drying MM based on a BRBP neural network

(1) Determine the inputs and outputs

In the experimental design, the steam content was set to 0.5 L/h to analyze the effect of pressure and temperature on moisture drying. Therefore, temperature $T$, pressure $P$, initial moisture content $W_0$, and drying time $t$ were selected as the input variables, and the ratio of rice moisture content to initial moisture content at a given time MR was used as the output variable.

(2) Sample point selection and division

The moisture content results at six-time points were recorded for each of the 25 sets of experiments. To comprehensively evaluate the effectiveness of the machine learning model algorithm, the model evaluation strategy was as follows: The six pieces of experimental data of the $i$-th set were selected as the test samples, and the test data of the other 24 sets were used as the training samples. Then, the BP neural network was trained; $i$ was set to 1, 2, 3,⋯, 25, and the model was trained 25 times and tested 25 times[29].

(3) Neural network topology and parameter selection

Corresponding to the built model, 4 traversals are input, and 1 variable is output. The neural network has 4 input nodes and 1 output node. According to the Kolmogorov theorem, a hidden layer with 20 hidden layer nodes is required. The transfer function was a sigmoid function, the output layer was a linear function, the maximum number of iterations was 1000, the training mean square error was 0, and the training speed was 0.05[30]. Some studies have shown that the BP neural network with the sigmoid function as the transfer function can approximate any continuous and bounded nonlinear function with arbitrary precision, even if the network has only one hidden layer.

3) Establishment of an MM for LPSS drying of paddy based on SVM[31]

(1) The inputs and outputs of the model are consistent with the input and output variables of the BRBP neural network model;

(2) The sample set division is consistent with that of the BRBP neural network model;

(3) The hyperparameters are selected using the regression SVM algorithm;

(4) $\varepsilon$ is the insensitive coefficient, with a parameter search space of ($1e^{-3}$, $1e^{2}$);

(5) $B$ is the penalty coefficient, with a parameter search space of ($1e^{-3}$, $1e^{3}$);

(6) $\gamma$ is the kernel width, with a parameter search space of ($1e^{-3}$, $1e^{3}$);

(7) The hyperparameter is optimized through the Bayesian optimization algorithm, with the 5-fold cross-validation error of the training samples as the optimization objective.

## 3 Results and discussion

### 3.1 Analysis of the characteristics of LPSS drying of paddy

Two representative sets of experimental data were selected for discussion and interpretation. One set of data was from the set of experiments at the same pressure (0.03 MPa) and different temperatures (50°C-70°C), and the other set of data was from the set of experiments at the same temperature (50°C) and different pressures (0.01-0.03 MPa). The time-dependent curves of the moisture content, drying rate, and MR of the paddy samples under different experimental conditions are shown in Figures 2-4, respectively.

Figure 2a shows the time-dependent curves of the paddy moisture content under the same temperature and different pressures. As shown in the figure, the paddy moisture content decreased over time. The pressure affects the paddy moisture content. Specifically, the lower the absolute pressure is (the higher the degree of vacuum is), the lower the paddy moisture content at the same drying time. This occurs because the drying efficiency of paddy, which is a porous thermosensitive medium, is higher at a lower pressure (larger degree of vacuum) as the lower pressure enhances the internal diffusion through porous particles and boosts water evaporation by lowering the boiling point of water. The formula for calculating the degree of superheating is $\Delta T_{sh}=T_o-T_{sat}$, where $T_o$ is the operating temperature, °C; $T_{sat}$ is the saturation temperature, °C; $\Delta T_{sh}$ is the degree of superheating. A lower operating pressure results in a lower saturation temperature $T_{sat}$. If the operating temperature remains unchanged, a higher degree of superheating is obtained, and the degree of superheating is considered an important parameter in the LPSS drying process[32,33].

Figure 2b shows the time-dependent curves of the paddy moisture content under the same pressure and different temperatures. As shown in the figure, the paddy moisture contents decrease with time, and the temperature has an evident impact on the paddy moisture content as the higher the temperature is, the lower the moisture content at the same drying time. This is attributed to a higher temperature leading to a faster water evaporation rate. The constant boiling point of water at constant pressure and higher temperature results in a higher degree of superheating and thereby a faster drying rate[34].

### 3.2 Empirical model fitting results and analysis

Table 2 shows the goodness of fit ($R^2$) between the experimental results and the five common thin-layer drying MMs (Henderson and Pabis model, Page model, Midilli model, logarithmic model, and Lewis model) under various drying conditions. The $R^2$ values of each model are listed in Table 2, and the effects of fitting between the data and the empirical MMs are shown in Figures 3-7.

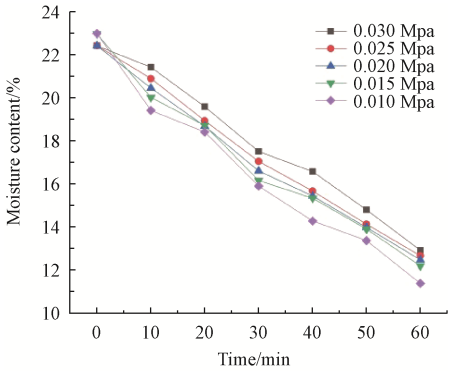


a. Under different pressures

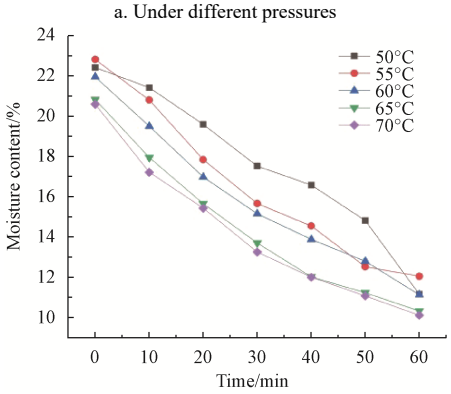


b. Under different temperatures

Figure 2 Variation of moisture content with time

Figures 3-7 show the goodness of fit ($R^2$) between the experimental results and the five common thin-layer drying MMs (Henderson and Pabis model, Page model, Midilli model, logarithmic model, and Lewis model) under various drying conditions.

Based on each individual experiment, the Henderson and Pabis model, the Page model, the Midilli model, and the logarithmic model produce good fitting results. Of them, the Midilli model shows the best fitting effect (maximum $R^2$: 0.9996, minimum $R^2$: 0.970), and the Lewis model has the worst fitting effect (minimum $R^2$: 0.7381).

**Table 2 Fitting results of five common thin-layer drying MMs**

| $T$ /°C | $P$ /MPa | $R^2$ | | | | |
|---|---|---|---|---|---|---|
| | | Hederson and Pabis[26-28] | Page [26-28] | Midilli [26-28] | Logarithmic [26-28] | Lewis [26-28] |
| 50 | 0.0100 | 0.9767 | 0.9606 | 0.9853 | 0.9850 | 0.9672 |
| 50 | 0.0150 | 0.9894 | 0.9834 | 0.9889 | 0.9884 | 0.9713 |
| 50 | 0.0200 | 0.9868 | 0.9894 | 0.9892 | 0.9875 | 0.9361 |
| 50 | 0.0250 | 0.9715 | 0.9919 | 0.9847 | 0.9808 | 0.9708 |
| 50 | 0.0300 | 0.9271 | 0.9865 | 0.9901 | 0.9670 | 0.8997 |
| 55 | 0.0100 | 0.9639 | 0.9689 | 0.9996 | 0.9980 | 0.9471 |
| 55 | 0.0150 | 0.9966 | 0.9963 | 0.9973 | 0.9965 | 0.9920 |
| 55 | 0.0200 | 0.9902 | 0.9895 | 0.9975 | 0.9975 | 0.9899 |
| 55 | 0.0250 | 0.9813 | 0.9764 | 0.9914 | 0.9840 | 0.9451 |
| 55 | 0.0300 | 0.9783 | 0.9802 | 0.9941 | 0.9940 | 0.9813 |
| 60 | 0.0100 | 0.9803 | 0.9801 | 0.9991 | 0.9989 | 0.9788 |
| 60 | 0.0150 | 0.9783 | 0.9908 | 0.9982 | 0.9944 | 0.8318 |
| 60 | 0.0200 | 0.9861 | 0.9942 | 0.9967 | 0.9955 | 0.9578 |
| 60 | 0.0250 | 0.9669 | 0.9707 | 0.9976 | 0.9976 | 0.9656 |
| 60 | 0.0300 | 0.9922 | 0.9934 | 0.9971 | 0.9943 | 0.9872 |
| 65 | 0.0100 | 0.9920 | 0.9918 | 0.9943 | 0.9933 | 0.9445 |
| 65 | 0.0150 | 0.9810 | 0.9915 | 0.9893 | 0.9867 | 0.7832 |
| 65 | 0.0200 | 0.9796 | 0.9852 | 0.9852 | 0.9817 | 0.7380 |
| 65 | 0.0250 | 0.9778 | 0.9656 | 0.9860 | 0.9858 | 0.8641 |
| 65 | 0.0300 | 0.9835 | 0.9946 | 0.9989 | 0.9983 | 0.9690 |
| 70 | 0.0100 | 0.9761 | 0.9906 | 0.9925 | 0.9926 | 0.9298 |
| 70 | 0.0150 | 0.9900 | 0.9962 | 0.9943 | 0.9940 | 0.9834 |
| 70 | 0.0200 | 0.9657 | 0.9750 | 0.9715 | 0.9673 | 0.8720 |
| 70 | 0.0250 | 0.9987 | 0.9981 | 0.9990 | 0.9989 | 0.9779 |
| 70 | 0.0300 | 0.9987 | 0.9950 | 0.9991 | 0.9991 | 0.9142 |

Note: $T$ is the drying temperature, °C; $P$ is the drying pressure, MPa. Same below.

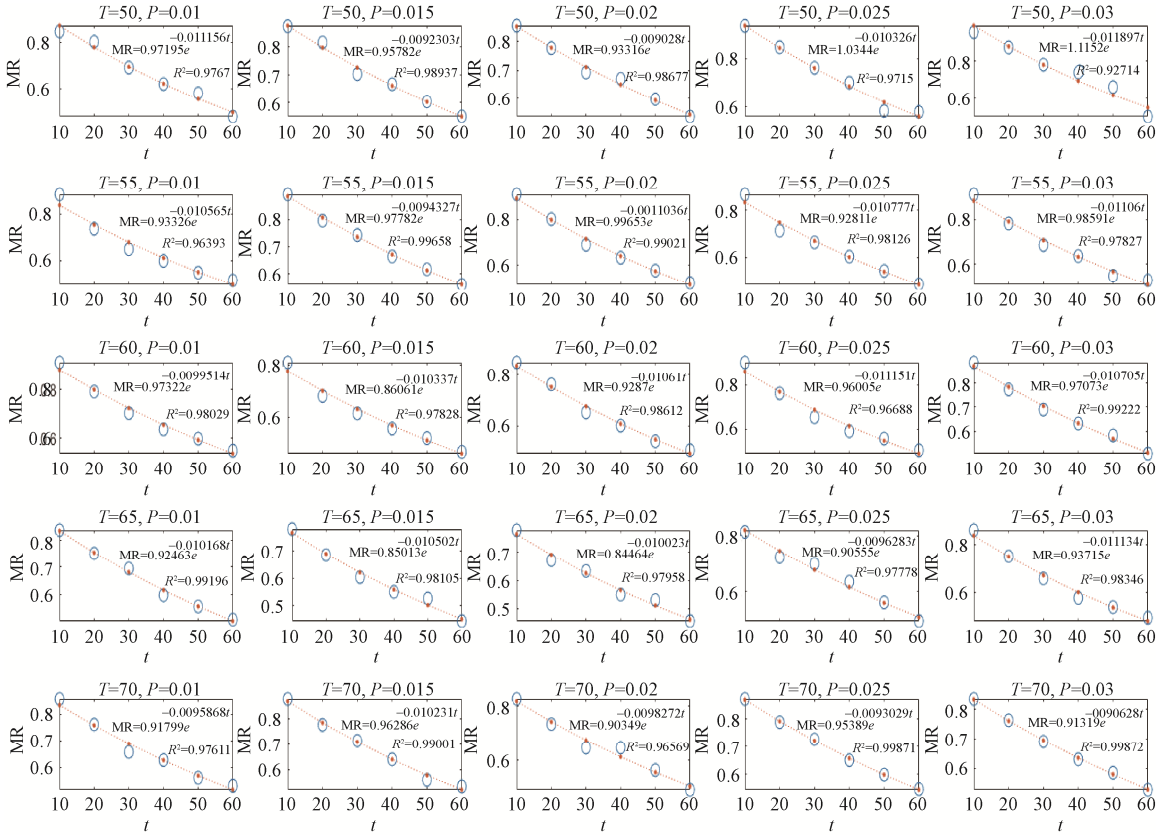


Note: MR is the moisture ratio of a paddy sample,%; $t$ is the drying time, s; $T$ is the drying temperature, °C; $P$ is the drying pressure, MPa. Same below.

Figure 3 Regression relationships between MR and $t$ under different experimental conditions based on the Henderson and Pabis model

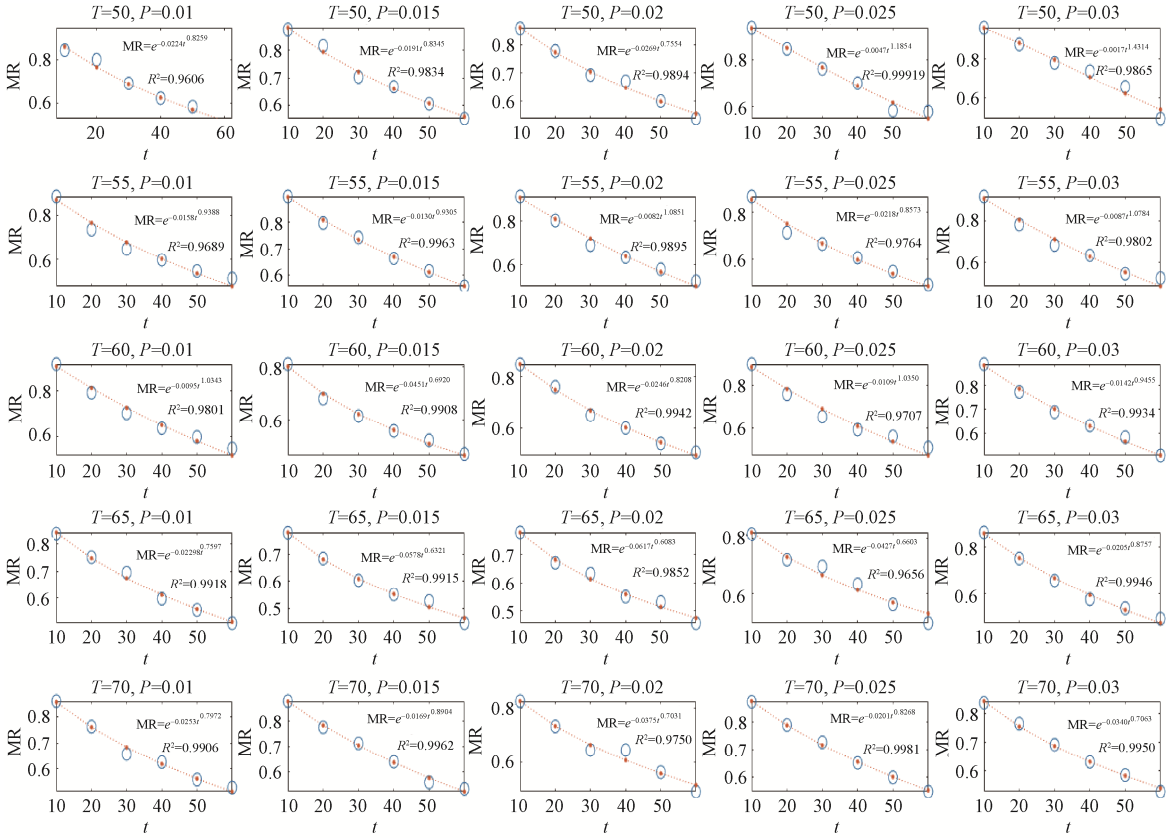


Figure 4 Regression relationships between MR and *t* under different experimental conditions based on the page model

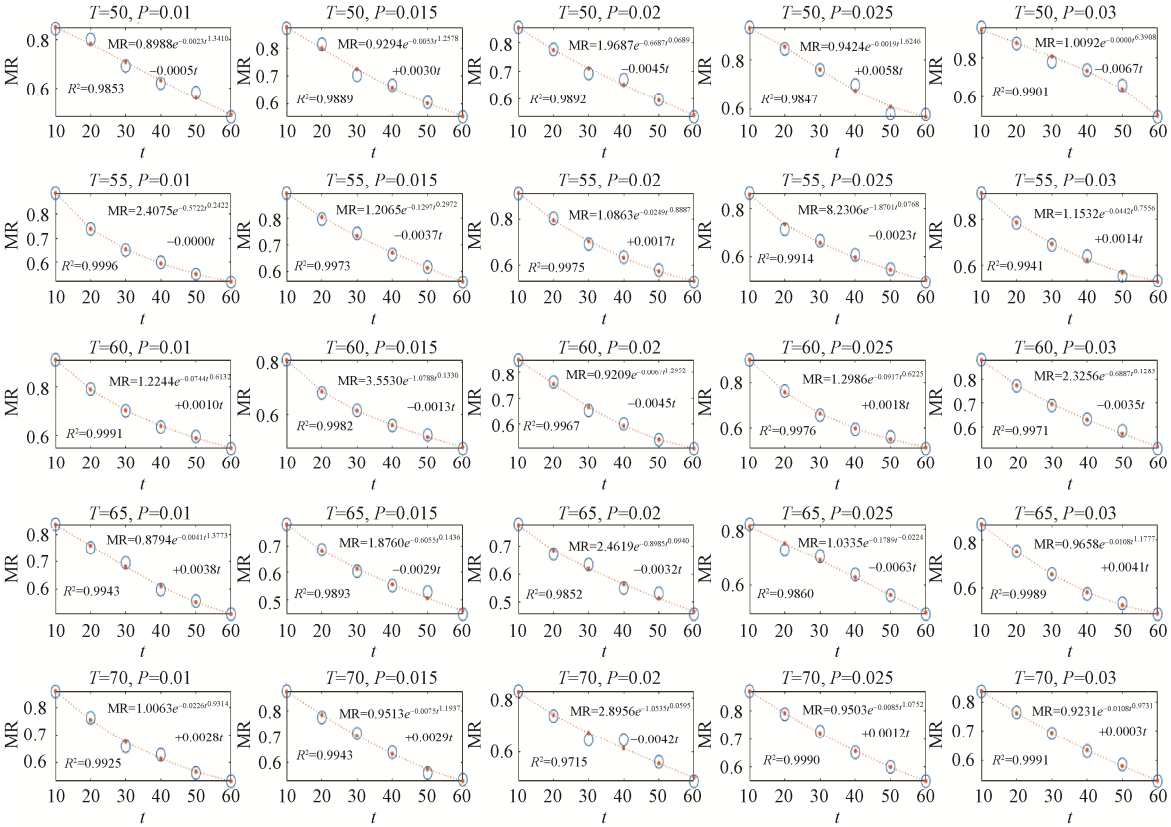


Figure 5 Regression relationships between MR and *t* under different experimental conditions based on the Midilli model

### 3.3 Regression fitting results of the coefficients of each model

According to the above-mentioned discussion, it can be concluded that each model has a great prediction under each individual experimental condition. But it was preferred to use one expression to predict results for all experimental conditions. Therefore, the coefficients of 25 expressions obtained from 25 groups of experiments of each model were fitted as a whole, and different experimental independent variables were used to calculate and express the coefficients. The results are listed in Table 3.

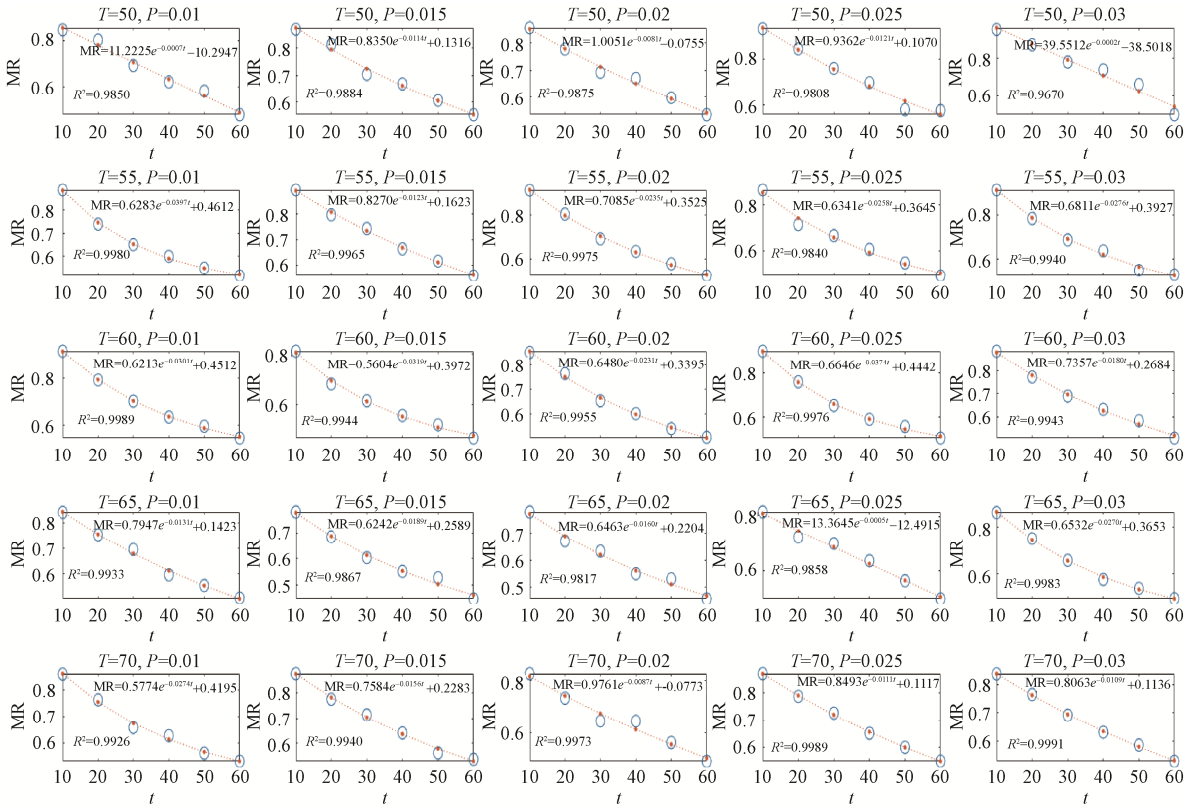


Figure 6 Regression relationships between MR and *t* under different experimental conditions based on the logarithmic model

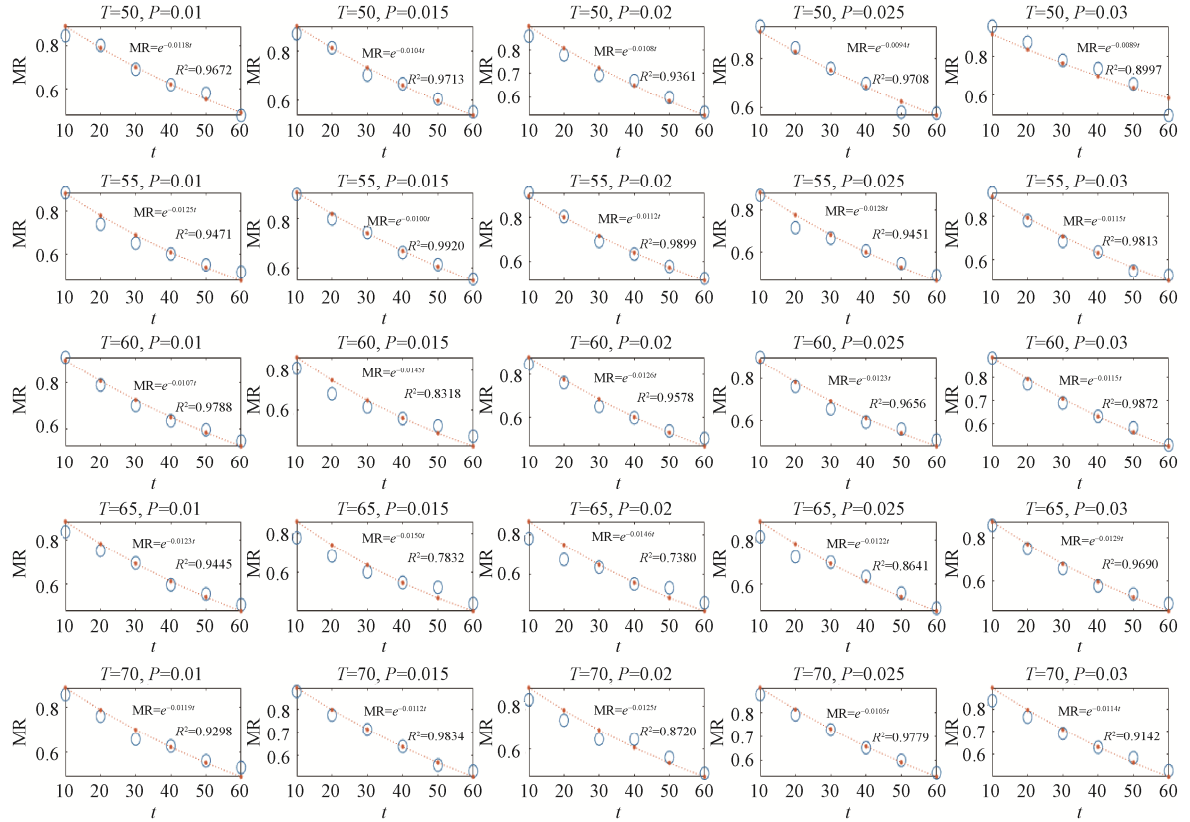


Figure 7 Regression relationships between MR and *t* under different experimental conditions based on the Lewis model

The equation and goodness of fit of each coefficient of the five common thin-layer drying MMs are obtained by calculating the model coefficient(s) of each model under each experimental condition and performing regression fitting. The five MMs can predict the MR at different times under a single experimental condition but have a poor fit for the overall experimental conditions. Hence, none of them can be used as the drying model for the experimental conditions in this study. Therefore, a more adaptive model construction method is necessary to accurately predict the MR under different drying conditions.

**Table 3 Regression fitting results of the coefficients of each model**

| Model name | Model equation | Expression of coefficient | $R^2$ |
|---|---|---|---|
| Hederson and Pabis | $MR = a\exp(-kt)$ | $a = 2.3345 - 0.0444T + 0.0004T^2 - 0.2506T \cdot P + 432.4688P^2$ | 0.6177 |
| | | $k = 0.0116 - 0.0008T + 0.0034T \cdot P - 5.6662P^2$ | 0.4035 |
| Page | $MR = \exp(-kt^x)$ | $k = 1.2020 - 0.7861T \cdot P + 1372.7241P^2$ | 0.5833 |
| | | $x = -0.0005 + 0.0551T \cdot P - 93.1454P^2$ | 0.3974 |
| Midilli | $MR = a\exp(-kt^x) + bt$ | $a = -0.0306 + 0.0010T + 0.3366P - 8.0295P^2$ | 0.1192 |
| | | $k = -0.0104 + 0.0003T + 0.1487P - 3067P^2$ | 0.1594 |
| | | $x = 0.0038 - 0.0001T - 0.0007T \cdot P - 1.1412P^2$ | 0.5010 |
| | | $b = 0.0040 - 0.5106P - 0.0007T^2 + 10.6793P^2$ | 0.0535 |
| Logarithmic | $MR = a\exp(-kt) + c$ | $a = 10.9677 - 20.9539T \cdot P + 38643P^2$ | 0.2562 |
| | | $k = -0.5418 + 0.0188T - 0.0002T^2$ | 0.3696 |
| | | $c = -9.8812 + 20.7313T \cdot P - 38277P^2$ | 0.2521 |
| Lewis | $MR = \exp(-kt)$ | $k = -0.0548 + 0.0022T - 0.0001T^2$ | 0.4163 |

### 3.3 BRBP neural network-based drying MM

According to the training and testing strategies in this study, the following results are obtained. 1) The test results are shown in Figure 8; 2) The training and testing accuracy and errors of the BRBP neural network-based drying MM are listed in Table 4.

The BRBP neural network-based drying MM has a mean training root mean square error (RMSE) of 0.019, a mean testing RMSE of 0.027, a mean training mean absolute error (MAE) of 0.069, a mean testing MAE of 0.044, a mean training $R^2$ of 0.974, and a mean testing $R^2$ of 0.940.

### 3.4 SVM-based drying MM

According to the training and testing strategies in this study, the following results are obtained. 1) The test results are shown in Figure 9; 2) The training and testing accuracy and errors of the SVM-based drying MM are listed in Table 5.

The SVM-based MM for paddy drying has a mean training RMSE of 0.025, a mean testing RMSE of 0.027, a mean training MAE of 0.081, a mean testing MAE of 0.048, a mean training $R^2$ of 0.957, and a mean testing $R^2$ of 0.942.

According to the modeling results based on the BRBP neural network and support vector machine with the fitting coefficients of the five empirical models in Table 3, the BRBP neural network-based MM is slightly better than the SVM-based MM in terms of training RMSE, testing RMSE, training MAE, testing MAE, training $R^2$, and testing $R^2$ and both are significantly better than the empirical MM (the Henderson and Pabis model). The results indicate that the MMs established by the two machine learning methods can better predict the moisture content of paddy during LPSS drying.

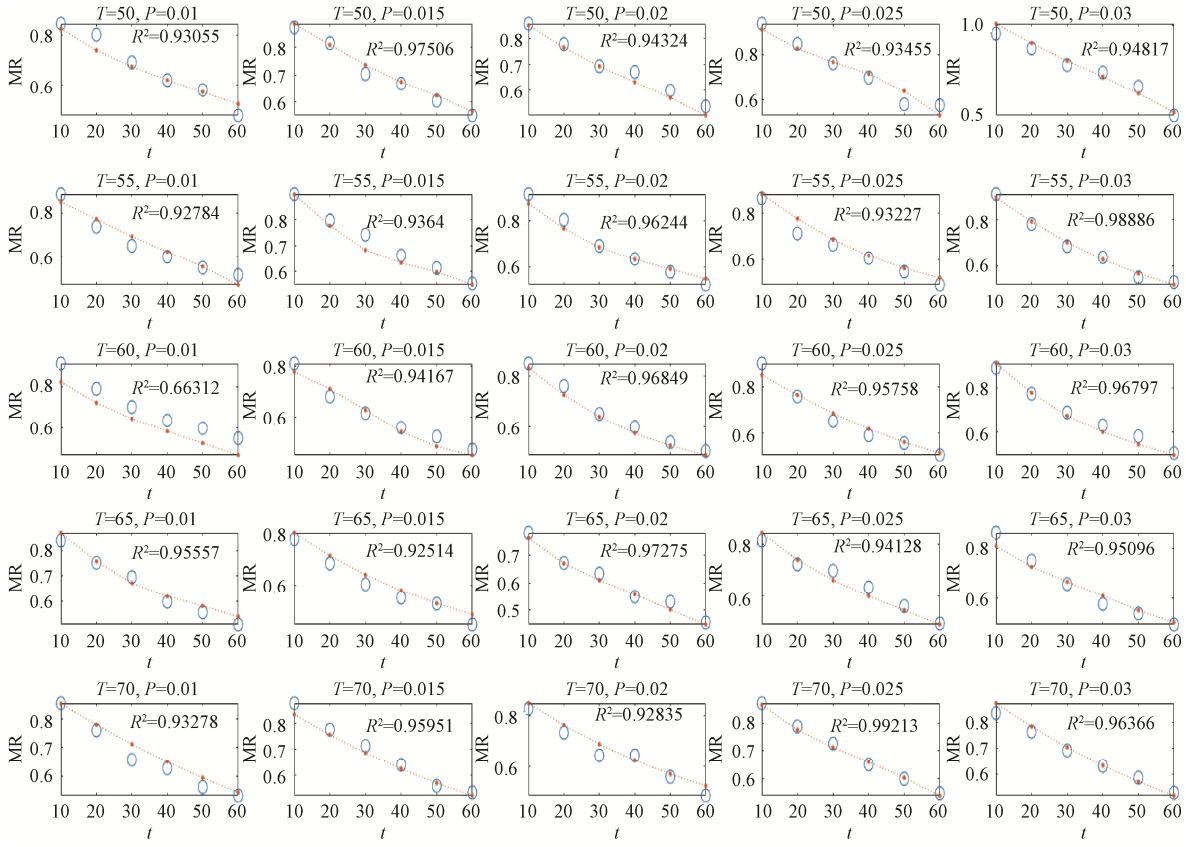


Figure 8 Test results of the BRBP neural network-based drying MM

**Table 4 Training and testing accuracies of the BRBP neural network-based drying MM**

| *T*/°C | *P*/MPa | Training RMSE | Test RMSE | Training MAE | Test MAE | Training $R^2$ | Testing $R^2$ |
|---|---|---|---|---|---|---|---|
| 50 | 0.01 | 0.0154 | 0.0331 | 0.0579 | 0.0613 | 0.9848 | 0.9306 |
| 50 | 0.015 | 0.0147 | 0.0176 | 0.0564 | 0.032 | 0.9862 | 0.9751 |
| 50 | 0.02 | 0.0152 | 0.0253 | 0.0495 | 0.0391 | 0.9855 | 0.9432 |
| 50 | 0.025 | 0.0148 | 0.0333 | 0.0895 | 0.0579 | 0.9859 | 0.9345 |
| 50 | 0.03 | 0.0169 | 0.0336 | 0.0889 | 0.055 | 0.9811 | 0.9482 |
| 55 | 0.01 | 0.0149 | 0.0338 | 0.051 | 0.0452 | 0.9858 | 0.9278 |
| 55 | 0.015 | 0.0147 | 0.029 | 0.0506 | 0.0593 | 0.9862 | 0.9364 |
| 55 | 0.02 | 0.015 | 0.0257 | 0.0612 | 0.0406 | 0.9855 | 0.9624 |
| 55 | 0.025 | 0.0143 | 0.0319 | 0.0425 | 0.0638 | 0.9869 | 0.9323 |
| 55 | 0.03 | 0.0274 | 0.014 | 0.0698 | 0.0175 | 0.9516 | 0.9889 |
| 60 | 0.01 | 0.0167 | 0.0714 | 0.0914 | 0.089 | 0.9822 | 0.6631 |
| 60 | 0.015 | 0.0191 | 0.027 | 0.1202 | 0.0392 | 0.9766 | 0.9417 |
| 60 | 0.02 | 0.0261 | 0.0215 | 0.0765 | 0.0353 | 0.9566 | 0.9685 |
| 60 | 0.025 | 0.0273 | 0.0275 | 0.072 | 0.0493 | 0.9522 | 0.9576 |
| 60 | 0.03 | 0.0147 | 0.0224 | 0.041 | 0.0366 | 0.9861 | 0.968 |
| 65 | 0.01 | 0.0147 | 0.0242 | 0.0397 | 0.0313 | 0.9862 | 0.9556 |
| 65 | 0.015 | 0.0274 | 0.0298 | 0.0831 | 0.0396 | 0.9517 | 0.9251 |
| 65 | 0.02 | 0.0166 | 0.0173 | 0.0577 | 0.0281 | 0.9823 | 0.9728 |
| 65 | 0.025 | 0.0158 | 0.0258 | 0.0749 | 0.037 | 0.9842 | 0.9413 |
| 65 | 0.03 | 0.0167 | 0.0281 | 0.1151 | 0.052 | 0.9821 | 0.951 |
| 70 | 0.01 | 0.0274 | 0.0293 | 0.0703 | 0.0555 | 0.9523 | 0.9328 |
| 70 | 0.015 | 0.0274 | 0.0243 | 0.0712 | 0.0435 | 0.9523 | 0.9595 |
| 70 | 0.02 | 0.0266 | 0.0294 | 0.0721 | 0.0443 | 0.955 | 0.9283 |
| 70 | 0.025 | 0.0149 | 0.0098 | 0.0458 | 0.0143 | 0.986 | 0.9921 |
| 70 | 0.03 | 0.0275 | 0.0199 | 0.0773 | 0.0383 | 0.9522 | 0.9637 |

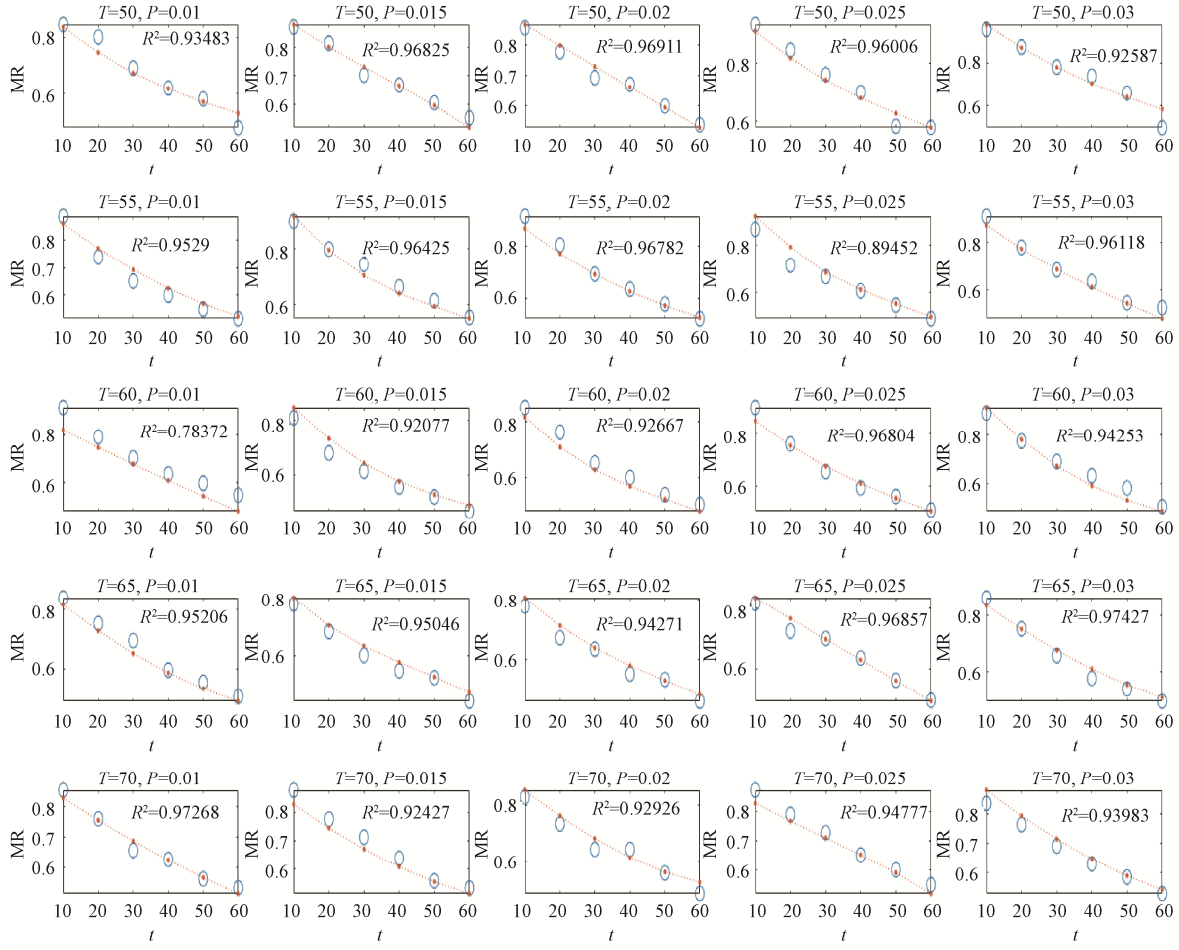


Figure 9 The test results of the SVM-based drying MM

**Table 5 Training and test accuracies of the SVM-based drying MM**

| $T$/°C | $P$ | Training RMSE | Test RMSE | Training MAE | Test MAE | Training $R^2$ | Training $R^2$ |
|---|---|---|---|---|---|---|---|
| 50 | 0.0100 | 0.0168 | 0.0321 | 0.0723 | 0.0548 | 0.9819 | 0.9348 |
| 50 | 0.0150 | 0.0180 | 0.0199 | 0.0718 | 0.0350 | 0.9794 | 0.9682 |
| 50 | 0.0200 | 0.0394 | 0.0187 | 0.0899 | 0.0370 | 0.9017 | 0.9691 |
| 50 | 0.0250 | 0.0241 | 0.0260 | 0.1035 | 0.0451 | 0.9623 | 0.9601 |
| 50 | 0.0300 | 0.0224 | 0.0402 | 0.0704 | 0.0874 | 0.9668 | 0.9259 |
| 55 | 0.0100 | 0.0276 | 0.0273 | 0.0833 | 0.0410 | 0.9511 | 0.9529 |
| 55 | 0.0150 | 0.0177 | 0.0217 | 0.0707 | 0.0399 | 0.9801 | 0.9642 |
| 55 | 0.0200 | 0.0257 | 0.0238 | 0.0890 | 0.0465 | 0.9575 | 0.9678 |
| 55 | 0.0250 | 0.0157 | 0.0399 | 0.0707 | 0.0776 | 0.9842 | 0.8945 |
| 55 | 0.0300 | 0.0231 | 0.0262 | 0.0814 | 0.0458 | 0.9656 | 0.9612 |
| 60 | 0.0100 | 0.0352 | 0.0572 | 0.0816 | 0.0943 | 0.9208 | 0.7837 |
| 60 | 0.0150 | 0.0224 | 0.0315 | 0.0882 | 0.0528 | 0.9680 | 0.9208 |
| 60 | 0.0200 | 0.0209 | 0.0328 | 0.0778 | 0.0542 | 0.9721 | 0.9267 |
| 60 | 0.0250 | 0.0257 | 0.0238 | 0.0919 | 0.0510 | 0.9576 | 0.9680 |
| 60 | 0.0300 | 0.0214 | 0.0300 | 0.0939 | 0.0499 | 0.9706 | 0.9425 |
| 65 | 0.0100 | 0.0279 | 0.0251 | 0.0763 | 0.0432 | 0.9507 | 0.9521 |
| 65 | 0.0150 | 0.0157 | 0.0242 | 0.0593 | 0.0307 | 0.9841 | 0.9505 |
| 65 | 0.0200 | 0.0193 | 0.0251 | 0.0716 | 0.0408 | 0.9761 | 0.9427 |
| 65 | 0.0250 | 0.0404 | 0.0189 | 0.0962 | 0.0416 | 0.8967 | 0.9686 |
| 65 | 0.0300 | 0.0289 | 0.0204 | 0.0898 | 0.0328 | 0.9464 | 0.9743 |
| 70 | 0.0100 | 0.0331 | 0.0186 | 0.0796 | 0.0309 | 0.9306 | 0.9727 |
| 70 | 0.0150 | 0.0307 | 0.0332 | 0.0797 | 0.0502 | 0.9397 | 0.9243 |
| 70 | 0.0200 | 0.0279 | 0.0292 | 0.0911 | 0.0398 | 0.9508 | 0.9293 |
| 70 | 0.0250 | 0.0167 | 0.0253 | 0.0687 | 0.0451 | 0.9823 | 0.9478 |
| 70 | 0.0300 | 0.0290 | 0.0256 | 0.0836 | 0.0450 | 0.9468 | 0.9398 |

## 4 Conclusions

1) The Bayesian regularization back propagation (BRBP) neural network-based drying mathematical model (MM) has a mean training root mean square error (RMSE) of 0.019, a mean testing RMSE of 0.027, a mean training mean absolute error (MAE) of 0.069, a mean testing MAE of 0.044, a mean training $R^2$ of 0.974, and a mean testing $R^2$ of 0.940, showing a good fitting effect;

2) The SVM-based paddy drying MM has a mean training RMSE of 0.025, a mean testing RMSE error of 0.027, a mean training MAE of 0.081, a mean testing MAE of 0.048, a mean training $R^2$ of 0.957, and a mean testing $R^2$ of 0.942, showing a good fitting effect;

3) The BRBP neural network-based MM is slightly better than the SVM-based MM in terms of training RMSE, testing RMSE, training MAE, testing MAE, training $R^2$, and testing $R^2$, and both are significantly better than the empirical MM (the Henderson and Pabis model). The results indicate that the MMs established by the two machine learning methods can better predict the moisture content of paddy during low-pressure superheated steam (LPSS) drying.

## [References]


[1] Karladee D, Suriyong S. γ-aminobutyric acid (GABA) content in different varieties of brown rice during germination. Science Asia, 2012; 38(1): 13–17.

[2] Zargarchi S, Saremnezhad S. Gamma-aminobutyric acid, phenolics and antioxidant capacity of germinated indica paddy rice as affected by low-pressure plasma treatment. LWT, 2019; 102: 291–294.

[3] Meyerhoff D J, Mon A, Metzler T, Neylan T C. Cortical gamma-aminobutyric acid and glutamate in posttraumatic stress disorder and their relationships to self-reported sleep quality. Sleep, 2014; 37(5): 893–900.

[4] Maric T T, Piantadosi P T, Floresco S B. Prefrontal cortical gamma-aminobutyric acid transmission and cognitive function: drawing links to schizophrenia from preclinical research. Biological psychiatry, 2015, 77(11): 929–939.

[5] Brady Jr R O, McCarthy J M, Prescot A P, Jensen J E, Cooper A J, Cohen B M, et al. Brain gamma-aminobutyric acid (GABA) abnormalities in bipolar disorder. Bipolar disorders, 2013; 15(4): 434–439.

[6] Benson K L, Bottary R, Schoerning L, Baer L, Gonenc A, Jensen J E, et al. 1 H MRS measurement of cortical GABA and glutamate in primary insomnia and major depressive disorder: Relationship to sleep quality and depression severity. Journal of Affective Disorders, 2020; 274: 624–631.

[7] Li Y, Che G, Wan L, Qu T Q, Zhang Q L, Zhao F Z. Effects of a combined processes of low-pressure steam enrichment and low-pressure superheated steam drying on the γ-aminobutyric acid content of *Japonica* rice. Journal of Chemistry, 2022; 2022: 8196654. doi: 10.1155/2022/8196654.

[8] Chungcharoen T, Prachayawarakorn S, Soponronnarit S, Tungtrakul P. Effect of drying temperature on drying characteristics and quality of germinated rices prepared from paddy and brown rice. Drying Technology, 2012; 30(16): 1844–1853.

[9] Sghaier J, El Ganaoui M, Chrusciel L, Gabsi S. Low-pressure superheated steam drying of a porous media. Drying Technology, 2015; 33(1): 103–110.

[10] Wang J C, Xu Q, Liu J B, Zheng S S, Wang R F, Li Z Y. Drying of pineapple slices using combined low-pressure superheated steam and vacuum drying. International Journal of Food Engineering, 2021; 17(11): 865–875.

[11] Sehrawat R, Nema P K, Chandra P. Quality evaluation of onion slices dried using low pressure superheated steam and vacuum drying. Journal of Agricultural Engineering, 2017; 54(3): 32–39.

[12] Liu J B, Xue J, Xu Q, Shi Y P, Wu L, Li Z Y. Drying kinetics and quality attributes of white radish in low pressure superheated steam. International Journal of Food Engineering, 2017; 13(7): 20160365. doi: 10.1515/ijfe-2016-0365.

[13] Sehrawat R, Nema P K, Kaur B P. Quality evaluation and drying characteristics of mango cubes dried using low-pressure superheated steam, vacuum and hot air drying methods. LWT, 2018; 92: 548–555.

[14] Pan Y K, Wang X Z, Liu X D. Modern drying technology-2nd Ed. Chemical Industry Press, 2007; pp.773–787.

[15] Devahastin S, Suvarnakuta P, Soponronnarit S, Mujumdar A S. A comparative study of low-pressure superheated steam and vacuum drying of a heat-sensitive material. Drying Technology, 2004; 22(8): 1845–1867.

[16] Martinello M A, Mattea M A, Crapiste G. Superheated steam drying of

parsley: A fixed bed model for predicting drying performance. Latin American applied research, 2003; 33(3): 333–337.

[17] Elustondo D, Elustondo M P, Urbicain M J. Mathematical modeling of moisture evaporation from foodstuffs exposed to subatmospheric pressure superheated steam. Journal of Food Engineering, 2001; 49(1): 15–24.

[18] Zhang X K, Sun R C, Wang X C, Su Z W, Cao W. Drying models and characteristics of thin layer sludege in superheated steam drying. Transactions so the CSAE, 2014; 30(14): 238–266. (in Chinese)

[19] Li Z Y, Liu J B, Xu Q, Shi Y P. Study on inversion temperature in low pressure superheated steam drying of green turnip slice. Transactions of the CSAE, 2018; 34(1): 279–286. (in Chinese)

[20] Yuan D L, Geng W G, Du R, Sun C F, Wang S Q, Zhao G J. Drying characteristics and modelling of of *Penaeus vannamei* during superheated steam drying. Food Science, 2020; 41(3): 62–67. (in Chinese)

[21] Zhu W X, Sun S H, Chen P T, Chen Z H. Moisture content prediction model of peony hot air drying based on BP neural network. Transactions of the CSAM, 2011; 42(8): 128–130, 137. (in Chinese)

[22] Bai J W, Tian X Y, Ma H L. BP neural network modeling to predict moisture content of grapes after air impingement drying. Modern Food Science and Technology, 2016; 32(12): 198–203. (in Chinese)

[23] Zhang B H, Qian C Q, Jiao J K, Ding Z H, Zhang Y, Cui H G, et al. Rice mosture content detection method based on dielectric properties and SPA-SVR algorithm. Transactions of the CSAE, 2019; 35(18): 237–244. (in Chinese)

[24] Jiang B. Study on modeling by support vector machine and fuzzy neural network control of wood drying. PhD dissertation. Harbin: Northeast Forestry University, 2015; 128p. (in Chinese)

[25] Huang X L. Mechanical characteristics and drying kinetics during superheated steam drying of rice kernel. PhD dissertation. Beijing: China Agricultural University, 2014; 108p. (in Chinese)

[26] Babalis S J, Papanicolaou E, Kyriakis N, Belessiotis V G. Evaluation of thin-layer drying models for describing drying kinetics of figs (*Ficus carica*). Journal of Food Engineering, 2006; 75(2): 205–214.

[27] Diamante L M, Munro P A. Mathematical modelling of the thin layer solar drying of sweet potato slices. Solar Energy, 1993; 51(4): 271–276.

[28] Chhinnan M S. Evaluation of selected mathematical models for describing thin-layer drying of in-shell pecans. Transactions of the ASAE, 1984; 27(2):610–615.

[29] Song F Y, Lu Y, Ling Y S, Yang X, Qi Y, Chen J, et al. Simulation of infrared transmittance of water vapor based on BP neural network. Journal of Optoelectronics·Laser, 2017; 28(4): 451–456. (in Chinese)

[30] Zhang S R, Li X K. An estimation algorithm of BP neural network hidden layer nodes based on simulated annealing. Journal of Hefei University of Technology (Natural Science Edition), 2017; 40(11): 1489–1491, 1506. (in Chinese)

[31] Yu C, Song J D, Li S Y. The in situ earthquake early warning based on support vector machine (SVM) peak ground motion prediction. Journal of vibration and shock, 2021; 40(3): 63–72, 80.

[32] Kozanoglu B, Flores A, Guerrero-Beltrán J A, Welti-Chanes J. Drying of pepper seed particles in a superheated steam fluidized bed operating at reduced pressure. Drying Technology, 2012; 30(8): 884–890.

[33] Suvarnakuta P, Devahastin S, Soponronnarit S, Mujumdar A S. Drying kinetics and inversion temperature in a low-pressure superheated steam-drying system. Industrial & Engineering Chemistry Research, 2005; 44(6): 1934–1941.

[34] Kozanoglu B, Vazquez A C, Chanes J W, Patiño J L. Drying of seeds in a superheated steam vacuum fluidized bed. Journal of Food Engineering, 2006; 75(3): 383–387.